Research Square

Preprints are preliminary reports that have not undergone peer review.
They should not be considered conclusive, used to inform clinical practice,
or referenced by the media as validated information.

# From Virtual Surgical Planning to Clinical Accuracy: A Proof-of-Principle Study of 3D- Printed Patient-Specific Drill and Placement Guides for Surgically Assisted Rapid Palatal Expansion

**Mario J.J. Scheurer**

mario.scheurer@uni-ulm.de

Military Hospital Ulm, Academic Hospital of the University of Ulm

**Johannes Schulze**

Military Hospital Ulm, Academic Hospital of the University of Ulm

**Tim Eisenmann**

Implantec Dental Laboratory GmbH

**Dieter Ehret**

Implantec Dental Laboratory GmbH

**Eleni Schramm**

University Hospital Ulm Albert-Einstein-Allee 10

**Marcel Ebeling**

Military Hospital Ulm, Academic Hospital of the University of Ulm

**Robin Kasper**

Military Hospital Ulm, Academic Hospital of the University of Ulm

**Lukas Greber**

Military Hospital Ulm, Academic Hospital of the University of Ulm

**Majeed Rana**

University Hospital Ulm

**Frank Wilde**

Military Hospital Ulm, Academic Hospital of the University of Ulm

**Alexander Schramm**

Military Hospital Ulm, Academic Hospital of the University of Ulm

**Andreas Sakkas**

Military Hospital Ulm, Academic Hospital of the University of Ulm

---

**Research Article**

**Keywords:** Surgically assisted rapid palatal expansion (SARPE), Virtual surgical planning (VSP), Patient-specific medicine, Additive manufacturing (AM), 3D accuracy, Orthognathic surgery

**Posted Date:** November 3rd, 2026

**DOI:** https://doi.org/10.21203/rs.3.rs-10647902/v1

**License:** This work is licensed under a Creative Commons Attribution 4.0 International License.
Read Full License

**Additional Declarations:** No competing interests reported.

## Abstract

# Purpose

Surgically assisted rapid palatal expansion (SARPE) requires accurate positioning of the distraction device to achieve controlled skeletal expansion while limiting dentoalveolar side effects. Conventional workflows remain technique-sensitive and depend largely on intraoperative judgement. This proof-of-principle study investigated the technical feasibility of a fully digital workflow integrating virtual surgical planning (VSP) with patient-specific drill and placement guides for a customized SARPE device and quantified the accuracy of transferring the planned device position to surgery in a single patient.

# Methods

VSP included device positioning and screw trajectory planning. Patient-specific drill guide and patient-specific placement guide were designed as dentition-supported, one-fit-only devices and additively manufactured. A hybrid patient-specific SARPE device was positioned using these guides. Transfer accuracy was evaluated by surface-based superimposition of the planned device geometry and its postoperative position and quantified.

# Results

Superimposition demonstrated close correspondence in the central palatal region containing the expansion screw, whereas the largest deviations occurred at the lateral fixation arms. Dice similarity coefficient was 0.17, the mean model-to-model surface distance was 2.78 mm, mean Hausdorff distance was 1.00 mm and maximum Hausdorff distance 5.70 mm.

# Conclusions

This fully digital workflow was technically feasible and successfully implemented. Although transfer appeared most accurate in the functionally decisive central region, peripheral deviations and limited global overlap preclude interpreting this single case as evidence of established accuracy. Cohort studies with predefined regional accuracy endpoints are needed to determine reproducibility, identify sources of error and assess whether the workflow provides clinically meaningful benefits over conventional SARPE device positioning.

## 1. Introduction

Transverse maxillary deficiency in skeletally mature patients represents an indication for Surgically Assisted Rapid Palatal Expansion (SARPE), particularly when orthopedic expansion alone is insufficient due to increased skeletal resistance of the midpalatal suture [1, 2]. SARPE aims to achieve controlled

skeletal widening of the maxilla while minimizing dentoalveolar side effects (e.g., buccal tipping, root resorption and periodontal compromise), which are commonly associated with purely tooth-borne expansion devices, particularly in periodontally compromised dentitions [3, 4].

Biomechanically, bone-borne or hybrid anchorage concepts have been shown to improve force transmission to the maxilla and reduce unwanted dental movements compared to conventional tooth-supported expanders. This is consistent with clinical observations demonstrating reduced dentoalveolar side effects and improved skeletal expansion patterns when forces are applied directly to the maxillary bone. However, currently available bone-borne distractors are often associated with increased surgical invasiveness, limited patient comfort and technique-sensitive intraoperative placement [4–7]. These findings support the concept of direct force transmission to the basal maxillary bone may reduce undesirable dental effects, although clinical outcomes remain influenced by device design and surgical technique.

From a surgical perspective, the outcome of SARPE is affected by the extent and configuration of osteotomies and adequate mobilization of maxillary resistance zones. Variations in surgical techniques have been associated with differences in expansion patterns, including asymmetric skeletal widening and heterogeneous dentoalveolar responses [6, 7]. In addition, factors related to expander design and surgical technique have been shown to influence expansion patterns, with asymmetric outcomes reported even under standardized conditions, suggesting that intraoperative device positioning may contribute to variability in treatment outcomes [8–10].

Despite ongoing refinements in surgical protocols and SARPE design, conventional SARPE workflows remain largely dependent on intraoperative judgment, which limits reproducibility and standardization [6, 7]. In recent years, digital workflows integrating virtual surgical planning (VSP), computer-assisted design and manufacturing (CAD/CAM) and patient-specific surgical guides have demonstrated improved accuracy in orthognathic surgery [11–13]. However, the application of VSP and computer-assisted surgery (CAS) to SARPE remains limited, as conventional SARPE protocols are predominantly based on established surgical techniques and analog approaches [7, 14, 15].

Against this background, the present proof-of-principle study introduces a fully digital workflow that integrates VSP with patient-specific, additively manufactured drill and placement guides for SARPE. This approach is designed to enable a precise and reproducible transfer of the preoperative plan to the intraoperative setting by linking three-dimensional (3D) virtual planning data directly to guided surgical execution. The primary objective of this study was to assess the technical feasibility and clinical applicability of this workflow, with particular emphasis on the accuracy of the intraoperative transfer of the VSP. By addressing these limitations of conventional SARPE procedures, this concept aims to reduce operator dependency and improve procedural consistency.

# 2. Materials and Methods

# 2.1 Study Design and Ethical Approval

**Ethical approval**

for this study was obtained from the ethics committee, University of Ulm (approval number: 131/25; approval date: August 6, 2025). This research was conducted in full accordance with the ethical standards of the institutional ethics committee and with the Helsinki declaration, respectively its later amendments [16]. For this proof-of-principle study, all data were anonymized and de-identified prior to analysis and written consent of the patient was obtained. Full compliance with data protection and safeguarding of data were ensured and no information which could identify the patient was collected. Reporting was based on the recommendations of the Strengthening the Reporting of Observational Studies in Epidemiology (STROBE) initiative [17].

# 2.2 Study Cohort

A 25-year-old male patient was treated at the Department of Oral and Plastic Maxillofacial Surgery, Military Hospital Ulm, presenting with a transverse maxillary deficiency with skeletal Class III dysgnathia and mandibular midline deviation and pronounced laterognathia. The patient had a history of completed orthodontic treatment during childhood and reported functional impairment, including difficulties in incisal biting and progressive temporomandibular joint symptoms. Clinical examination revealed a marked skeletal and dental Class III relationship with a retrognathic maxilla, anterior edge-to-edge bite (overjet – 2 mm, overbite 0 mm) and an unilateral posterior crossbite associated with transverse maxillary constriction and mandibular asymmetry.

Based on the clinical and radiological findings, the patient was scheduled for SARPE with transverse maxillary distraction using a bone-borne distraction device.

# 2.3 High-resolution 3D-imaging

Pre- and postoperative imaging was performed using cone-beam computed tomography (CBCT) (Axeos, Sirona Dental Systems GmbH, Bensheim, Germany). Image acquisition was conducted with a dentomaxillofacial field of view, enabling high-resolution 3D visualization of the maxillary complex. The CBCT datasets were reconstructed with isotropic submillimetric voxel sizes, allowing precise evaluation of osseous structures and their spatial relationships (i.e., dentition, dental roots, course infraorbital nerve) for surgical planning. Imaging demonstrated a transverse maxillary deficiency in the context of skeletal dysgnathia, characterized by a constricted maxillary arch and associated occlusal discrepancies.

# 2.4 Intraoral Scanning

Intraoral digital impressions were acquired using a hyperspectral, multi-modal imaging scanner (TRIOS 6, 3Shape, Copenhagen, Denmark). Full-arch scans of the maxilla and mandible, including occlusal registration, were obtained following a standardized scanning protocol. These datasets were merged

with CBCT data to generate a comprehensive virtual 3D model of the maxilla, serving as the basis for fully digital VSP.

## 2.5 Digital Workflow for Virtual SARPE Planning

### 2.5.1 Data Processing

Preoperative CBCT datasets of the midface were acquired and exported in Digital Imaging and Communications in Medicine (DICOM) format. Intraoral scans were obtained as Standard Tessellation Language (STL) files. Both datasets were imported into dedicated planning software (coDiagnostiX®, Dental Wings GmbH, Chemnitz, Germany) to enable multimodal data fusion.

Registration of CBCT and intraoral scan data was performed using surface-based matching of dental structures, allowing precise alignment of hard tissue anatomy with high-resolution dental surface information. This fused dataset served as the basis for subsequent virtual surgical planning.

### 2.5.2 Virtual SARPE Planning

Following data integration, a patient-specific 3D model of the maxilla was generated. Virtual planning of the SARPE device was performed according to a backward-planning concept, defining the spatial positioning of the SARPE device and fixation screws (Fig. 1) [18]. Special attention was given to the anatomical constraints of the maxilla, including tooth roots and alveolar bone morphology.

The virtual workflow comprised the following steps:

- Anatomical assessment of the maxillary bone and adjacent critical structures
- Virtual positioning of the expansion device in relation to the palatal vault
- Planning of screw trajectories with respect to root positions and cortical bone availability
- Verification of implant positioning in multiplanar CBCT views

This planning approach ensured anatomically guided and biomechanically optimized positioning of the SARPE device.

### 2.5.3 Computer-Aided Design and Manufacturing of Patient-Specific Models and Guides

Based on the finalized virtual plan, patient-specific drill guides (PSDG; Fig. 2) and patient-specific placement guides (PSPG; Fig. 3) were designed using CAD/CAM technology. The guide design was directly derived from the planned implant positions and screw trajectories, enabling accurate intraoperative transfer of the VSP.

PSDG and PSPG geometry were precisely adapted to the patient-specific anatomy to ensure stable and reproducible intraoperative seating. Emphasis was placed on a dentition-supported one-fit-only design, in

which the guide is uniquely constrained by the maxillary dentition [19, 20]. PSDG incorporated replaceable titanium drill sleeves (Steco-System-Technik GmbH & Co. KG, Hamburg, Germany), corresponding to the planned screw diameters and lengths as defined in the VSP [21].

## 2.6 Additive Manufacturing of Patient-Specific Models and Guides

Patient-specific physical maxillary dentition models (PSPMDM; Figs. 2 & 3), PSDG and PSPG were fabricated using additive manufacturing (AM). The PSPMDM was produced in transparent material (MED610, Stratasys, Eden Prairie, USA) to enable visualization of the underlying anatomical structures. Dentition and tooth roots were selectively rendered in opaque white material (Vero Pure White, Stratasys, Eden Prairie, USA) to enhance spatial orientation and to facilitate preoperative assessment of screw positioning in relation to dental root anatomy.

To further evaluate the feasibility of screw insertion under clinical conditions, a physical model of the head of a 90° angled screwdriver (MODUS 2, Medartis, Basel, Switzerland) was generated. This component was digitized using an intraoral scanner (TRIOS 6, 3Shape, Copenhagen, Denmark) and subsequently manufactured using the same additive manufacturing workflow, allowing simulation of intraoperative accessibility and angulation constraints.

In addition, the PSDG were designed as segmented guides, separated into right and left maxillary components (quadrants I and II), to improve intraoperative handling, accessibility and positioning accuracy (Fig. 3).

All components were manufactured using a multimaterial printer (DentaJet J5, Stratasys, Eden Prairie, USA), enabling the simultaneous fabrication of structures with distinct optical properties within a single model. Following printing, all models and guides underwent standardized post-processing procedures, including support removal and cleaning, prior to clinical application.

## 2.7 Manufacturing of the Patient-Specific SARPE Device

The patient-specific SARPE device (PSSD; Fig. 3) was manufactured using a hybrid design that combined a commercially available titanium expansion screw (Titan hyrax®, Dentaurum GmbH & Co. KG, Ispringen, Germany) with individually contoured 1.0 mm mini locking plates (DePuy Synthes, Zuchwil, Switzerland). In accordance with the manufacturer's instructions, the retention arms were adapted and rigidly connected to the palatal anchorage components. These connections were achieved by precision laser welding, ensuring a stable, durable and mechanically reliable assembly.

Device positioning followed established biomechanical principles. The expansion screw was aligned parallel to the occlusal plane to avoid lever effects and positioned with a clearance of approximately 1–2 mm from the palatal mucosa. Furthermore, the expansion screw was oriented in line with the mesio-palatal cusps of the first molars to ensure functional activation and accessibility of the activation key (Dentaurum GmbH & Co. KG, Ispringen, Germany).

## 2.8 Stepwise Surgical Procedure

The procedure was performed under general anesthesia in accordance with institutional standards for perioperative antimicrobial prophylaxis and sterile preparation.

### 2.8.1 Step 1: Guided Osteosynthesis Preparation Using Patient-Specific Drill Guides

PSDG were inserted sequentially on a quadrant-by-quadrant basis. PSDG demonstrated accurate dentition-supported seating with high positional stability (Fig. 4). Transmucosal guided drilling was performed in accordance with the predefined VSP protocol using a 1.5-mm angled drill system (Fig. 4).

### 2.8.2 Step 2: Guided Insertion of the Patient-Specific SARPE Device

Following removal of the PSDG, the PSSD device was inserted using a 3D-printed PSPG (Fig. 5). Dentition-supported PSPG demonstrated accurate dental and PSSP fit and facilitated precise PSSP positioning according to the VSP.

Fixation of the PSSP was achieved using locking screws (diameter 2.0 mm, length 10–12 mm; DePuy Synthes, Zuchwil, Switzerland), resulting in stable osteosynthetic anchorage at the palatal vault.

### 2.8.3 Step 3: Surgically Assisted Maxillary Osteotomies

A vestibular incision was made from region 16 to 26. Following elevation of a mucoperiosteal flap, the anterior maxillary wall, the zygomaticomaxillary buttress and the infraorbital nerve were exposed. Subperiosteal mobilization of the nasal floor and septum was performed. Horizontal osteotomy lines were marked bilaterally at the Le Fort I level and osteotomies were carried out symmetrically on both sides. Subsequently, a median osteotomy was performed in the region of teeth 11/21 using piezoelectric instrumentation (Mectron Medical Technology, Carasco, Italy) in combination with chisels.

### 2.8.4 Step 4: Functional Verification of Expansion

Trial activation of the PSSP was performed up to approximately 4 mm (20 turns × 0.2 mm). Symmetrical lateralization of the maxillary segments was achieved, accompanied by the formation of a midline diastema. The device was subsequently returned to its initial position.

### 2.8.5 Step 5: Wound Closure

A V-Y advancement flap was used for upper lip lengthening using resorbable sutures (Vicryl 4 – 0, Ethicon, Sint-Stevens-Woluwe, Belgium).

## 2.9 Postoperative 3D Accuracy Analysis

Postoperative accuracy of PSSD positioning was assessed using a standardized 3D image analysis workflow [22].

Preoperative VSP data (coDiagnostiX®, Dental Wings GmbH, Chemnitz, Germany), postoperative CBCT datasets and intraoral scan data were imported into open-source software (3D Slicer, version 5.10.0; released November 10th, 2025) for segmentation, registration and quantitative 3D analysis [23].

A two-step image registration protocol was applied to align all datasets within a common coordinate system. First, the preoperative CBCT dataset was aligned with the postoperative CBCT using an initial manual approximation followed by automated rigid registration (BRAINSFit algorithm). Subsequently, the intraoral scan was registered to the postoperative CBCT using surface-based matching of dental structures, enabling high-resolution assessment of the dental and device-related interfaces. The planned implant positions (including screw trajectories) were then aligned with the corresponding postoperative PSSP and screw positions.

Segmentation of the postoperative PSSD components was performed using a threshold-based approach to isolate metallic structures, followed by manual refinement to exclude adjacent bone. The resulting segmentation was converted into a 3D surface model representing the intraoperatively achieved implant configuration.

Rigid surface registration between the planned and postoperative models was performed using 3D Slicer's model registration module to determine the spatial relationship between planned and achieved PSSD positioning.

Quantitative deviation analysis was conducted using the Model-to-Model Distance module. Point-to-surface distances between the planned and postoperative models were calculated, generating color-coded deviation maps to visualize spatial discrepancies. In addition, angular deviations of screw trajectories were assessed using principal axis analysis.

Accuracy was evaluated using three complementary geometric metrics:

- Dice similarity coefficient (DSC):

DSC was used to quantify volumetric overlap between planned and postoperative implant geometries. It is defined as twice the intersection volume divided by the sum of both volumes. Values range from 0 (no overlap) to 1 (complete congruence), reflecting spatial agreement.

- Model-to-model surface distance (M2M):

M2M distance quantified mean geometric deviation between planned and achieved positions. For each surface point, the shortest Euclidean distance to the corresponding opposing surface was calculated. Lower values indicate higher geometric accuracy.

- Hausdorff distance (HD):

HD was used to determine the maximum surface deviation between planned and postoperative models. It represents the largest of all shortest point-to-surface distances and reflects the worst-case local discrepancy.

## 3. Results

## 3.1 Study Cohort

This proof-of-principle study included a single case presenting with transverse maxillary deficiency requiring SARPE using a PSSD. Treatment was performed at the Department of Oral and Plastic Maxillofacial Surgery, Military and University Hospital Ulm, Germany.

The indication for surgery was based on a skeletally determined transverse discrepancy that could not be adequately compensated by orthodontic treatment alone. Preoperative planning was performed using a fully digital workflow, incorporating CBCT and intraoral scan data for VSP, followed by CAD-based design of PSDG, PSPG and manufacturing of a hybrid PSSD.

## 3.2 Clinical Follow-Up

Postoperative follow-up (4 months) included standardized clinical assessments focusing on functional outcome, device stability and potential complications. The postoperative course was uneventful. Wound healing was regular, with no signs of infection, dehiscence or implant-related complications. Sensory function in the distribution of the infraorbital nerve remained intact. The device demonstrated stable anchorage throughout the observation period, with no signs of loosening or mechanical failure. At follow-up, the patient remained clinically stable with satisfactory functional outcome and no need for revision surgery.

## 3.3 Accuracy Analysis of Patient-Specific SARPE Device Positioning

Postoperative 3D accuracy analysis was performed using CBCT-based evaluation combined with intraoral surface registration to assess the spatial relationship between the virtually planned and the postoperative achieved PSSD position (Fig. 6).

## 3.3.1 Qualitative Assessment

Superimposition of the preoperative VSP and postoperative datasets demonstrated a high overall concordance between the planned and achieved PSSD positioning (Fig. 7). The central expansion screw region exhibited a high degree of positional accuracy, whereas deviations were primarily observed at the lateral anchorage arms. Color-coded surface distance maps revealed a non-uniform distribution of deviations, with increasing discrepancies toward the lateral maxillary regions, particularly in the anterior region of the second quadrant.

## 3.3.2 Quantitative Accuracy Analysis

This analysis demonstrated a measurable geometric correspondence between the virtually planned and the postoperative PSSD position (Table 1), with region-dependent variability in positional accuracy (Table 1). MSD was 2.78 mm, indicating a moderate global surface deviation between planned and achieved device position. In line with the qualitative assessment, lower deviations were observed in the central palatal region, reflecting accurate transfer of the planned distraction vector. Surface-based analysis using HD revealed a mean deviation of 1.00 mm and a maximum deviation of 5.70 mm, indicating overall low average discrepancies with localized peak deviations.

Volumetric agreement, expressed by DSC, was 0.17, reflecting limited volumetric overlap between planned and postoperative PSSD positions. Rigid transformation analysis demonstrated a total translational deviation [Distance between centers (DBC)] of 2.21 mm, with axis-specific components of -0.01 mm (X-axis), 0.57 mm (Y-axis) and 2.14 mm (Z-axis), indicating a predominant displacement along the vertical axis. Rotational deviation (RD) amounted to 6.19° (roll), 6.57° (pitch) and 2.72° (yaw), suggesting moderate angular discrepancies between planned and achieved PSSD orientation.

Table 1
Quantitative 3D accuracy analysis of PSSD placement: Volumetric, surface-based and rigid transformation metrics comparing VSP and postoperative PSSD positioning.

| Category | Measurement | Value |
|---|---|---|
| Volumetric metrics | | |
| | Dice similarity coefficient (DSC) [%] | 0.17 |
| | Mean surface distance (MSD) [mm] | 2.78 |
| Surface-based metrics | | |
| | Hausdorff distance (HD) [mm] | |
| | Mean | 1.00 |
| | Maximum | 5.70 |
| Translational and rotational metrics | | |
| | Distance between centers (DBC) [mm] | |
| | X | -0.01 |
| | Y | 0.57 |
| | Z | 2.14 |
| | Total | 2.21 |
| | Rotational deviation (RD) [°] | |
| | X (roll) | 6.19 |
| | Y (pitch) | 6.57 |
| | Z (yaw) | -2.72 |

# 4. Discussion

The present proof-of-principle study demonstrates the technical feasibility of a fully digital workflow integrating VSP for SARPE. This finding is consistent with previous work in orthognathic surgery, where CAD/CAM-based guides and patient-specific osteosynthesis have been shown to enable highly accurate plan transfer with reduced operator dependency [13, 22].

# 4.1 Interpretation of 3D Accuracy Findings

Quantitative analysis in the present study demonstrated a MSD of 2.78 mm, with a mean HD of 1.00 mm and a maximum deviation of 5.70 mm. These values indicate a moderate overall geometric deviation with localized peak discrepancies. Importantly, the spatial distribution of these deviations was non-

uniform and predominantly confined to the lateral fixation structures, whereas the central region demonstrated high positional concordance. This pattern is biomechanically plausible and clinically relevant. The central palatal region represents the functional core of PSSD, where accurate positioning directly determines the vector and symmetry of maxillary expansion. In contrast, the lateral fixation arms are subject to increased anatomical variability, including differences in soft tissue thickness, palatal curvature and screw trajectory constraints. Similar region-dependent variability has been reported in other patient-specific implant applications, particularly in anatomically complex regions such as the orbit, where deviations are often localized at peripheral implant extensions rather than central reference structures [24]. The observed DSC of 0.17 reflects limited volumetric overlap between planned and postoperative PSSD geometry. However, this metric must be interpreted with caution. As previously demonstrated, overlap-based metrics such as DSC are highly sensitive to small positional deviations in thin or elongated structures and may underestimate geometric agreement in such configurations [25, 26]. Therefore, surface-based metrics such as MSD and HD might be considered more appropriate for evaluating accuracy in non-volumetric implant geometries. Rigid transformation analysis revealed a total translational deviation of 2.21 mm, predominantly along the vertical axis and rotational deviations of up to 6.57°. These findings suggest that deviations were not random but followed a systematic pattern, likely related to intraoperative seating of the device and soft tissue interaction. Comparable systematic deviations have been described in template-guided dental implant placement, where minor discrepancies may arise from guide seating, manufacturing tolerances and intraoperative handling [21].

## 4.2 Comparison of Conventional SARPE with Digital SARPE Workflows

Conventional SARPE procedures are characterized by a high degree of intraoperative variability, particularly with respect to osteotomy design and device positioning. Several studies have demonstrated that expansion patterns may be asymmetric even under standardized conditions, suggesting that intraoperative factors play a critical role in treatment outcome [8, 9]. The present digital workflow addresses this limitation by directly linking preoperative planning with template-guided intraoperative execution. In contrast to conventional approaches, where screw placement and device positioning are performed freehand, the use of dental-supported, additively manufactured PSDG and PSPG enables predefined control of screw trajectories and SARPE device positioning. This concept is analogous to established computer-assisted workflows in orthognathic surgery, which have demonstrated improved reproducibility and accuracy compared to conventional techniques [11, 13, 22, 27]. In orthodontics, recent developments such as virtually planned Miniscrew-Assisted Rapid Palatal Expansion (MARPE) systems also aim to improve expansion control. However, these approaches primarily focus on appliance design rather than surgical guidance and therefore do not fully address the variability associated with intraoperative device placement and maxillary expansion [14]. The present study extends this concept by integrating surgical guidance into this workflow, thereby enabling a comprehensive digital treatment pathway.

## 4.3 Clinical Relevance

From a clinical perspective, the most relevant finding is the high positional accuracy in the central region. This suggests that the planned distraction vector might be reliably transferred to the patient, which is critical for achieving symmetrical skeletal expansion. Furthermore, the absence of intraoperative complications and the stable postoperative course, without hyperplasia of the palatal mucosa or overgrowth of the PSSD, support the clinical feasibility and safety of the presented approach. The ability to perform SARPE with predefined screw trajectories and implant positioning may reduce the risk of iatrogenic root injury and improve reproducibility, particularly in this anatomically challenging topography [28]. Additionally, template-guided drilling in combination with locking screws and plates allows for orthogonal alignment of screw trajectories even within the anatomically constrained palatal vault [29]. This may help to reduce unintended compression of the PSSD against the palatal mucosa associated with non-orthogonal insertion of the locking screws, which can lead to impingement of the SARPE device on the palatal soft tissues. Even small angular deviations may result in amplified positional discrepancies at the screw tip and shaft, what may affect the positioning of SARPE devices. Given the anatomical variability of the palatal vault, non-orthogonal screw insertion may therefore contribute to unintended positional discrepancies of the device relative to the palatal mucosa. This could be clinically relevant, as SARPE device-associated mucosal hyperplasia may impair patient comfort. Collectively, the presented workflow may contribute to improved patient compliance and tolerance of the therapy.

## 4.4 Limitations

Several limitations must be acknowledged. First, this study represents a proof-of-principle investigation based on a single case. Consequently, no statistical analysis or generalizable conclusions can be drawn. Second, the accuracy analysis is influenced by segmentation and registration processes, which are known sources of error in 3D image analysis [30]. Third, the use of CBCT data introduces inherent limitations in spatial resolution and artifact susceptibility, particularly in the presence of metallic structures. In addition, the DSC metric is of limited interpretability in this context, as discussed above. Future studies should therefore prioritize surface-based and transformation-based metrics when evaluating implant accuracy.

## 4.5 Future Perspectives

Future research should focus on prospective studies with larger patient cohorts to validate the clinical benefits of this workflow. Correlations between device positioning accuracy, expansion symmetry and long-term stability should be investigated. Moreover, integration with intraoperative imaging or navigation could further enhance accuracy, although this must be balanced against increased complexity and resource requirements. The presented concept also provides a foundation for further development of fully patient-specific SARPE devices, potentially incorporating additively manufactured monolithic designs with optimized biomechanical properties.

# 5. Conclusions

In conclusion, the present findings support the hypothesis that a fully digital, template-guided workflow enables accurate and reproducible transfer of VSP to SARPE procedures. While measurable deviations were observed, these were predominantly localized and did not affect the functionally relevant components of the device. The results are consistent with existing literature on CAS and patient-specific implants and highlight the potential of digital workflows to improve precision and standardization in SARPE.

## Abbreviations

AM
Additive manufacturing
CAD/CAM
Computer-aided design/Computer-aided manufacturing
CAS
Computer-assisted surgery
CBCT
Cone-beam computed tomography
CT
Computed tomography
DBC
Distance between centers
DICOM
Digital Imaging and Communications in Medicine
DSC
Dice similarity coefficient
HD
Hausdorff distance
MARPE
Miniscrew-Assisted Rapid Palatal Expansion
mm
Millimeter(s)
M2M
Model to model surface distance
PSDG
Patient-specific drill guide
PSI
Patient-specific implant
PSPG
Patient-specific placement guide
PSPMDM

Patient-specific physical maxillary dentition model
PSSD
Patient-specific SARPE device
RD
Rotational deviation
SARPE
Surgically Assisted Rapid Palatal Expansion
STL
Standard Tessellation Language
VSP
Virtual surgical planning
3D
Three-dimensional

## Declarations

**Ethics approval and consent to participate:**

The study was conducted in accordance with the Declaration of Helsinki and approved by the Ethics Committee of the University of Ulm (approval number: 131/25; date of approval: August 6, 2025). All data were anonymized and de-identified prior to analysis and written informed consent was obtained from the patient to participate.

**Consent for publication:**

Written informed consent was obtained from the patient for publication of the anonymized clinical data and accompanying images included in this manuscript.

# Competing interests:

The authors declare that they have no competing interests.

# Informed consent

**statement**: Informed consent was obtained from the patient of this study.

# Funding:

This research received no external funding. The APC was funded by University Ulm.

# Author Contribution

Conceptualization, M.S. and A.Sa.; methodology, J.S., T.E., D.E. and M.S.; software, J.S. and T.E.; validation, R.K. and L.G.; formal analysis, F.W. and A.Sc.; investigation, M.S. and J.S.; resources, M.S.; data curation, M.S. and J.S.; writing, original draft preparation, M.S.; writing, review and editing, R.K., L.G., M.E., E.S., M.R., F.W., A.Sc., A.Sa. and J.S.; visualization, M.S. and J.S.; supervision, M.S.; project administration, M.S. All authors reviewed and approved the final manuscript.

# Acknowledgements:

Not applicable.

**Clinical trial number**: Not applicable.

# Availability of data and materials:

The data supporting the findings of this study are included in the article.

## References

1. Bays RA, Greco JM. Surgically assisted rapid palatal expansion: An outpatient technique with long-term stability. J Oral Maxillofac Surg. 1992;50(2):110–3.
2. Betts NJ, Vanarsdall RL, Barber HD, Higgins-Barber K, Fonseca RJ. Diagnosis and treatment of transverse maxillary deficiency. Int J Adult Orthodon Orthognath Surg. 1995;10(2):75–96.
3. Seeberger R, Kater W, Schulte-Geers M, Davids R, Freier K, Thiele O. Changes after surgically-assisted maxillary expansion (SARME) to the dentoalveolar, palatal and nasal structures by using tooth-borne distraction devices. Br J Oral Maxillofac Surg. 2011;49(5):381–5.
4. Garib DG, Henriques JF, Janson G, de Freitas MR, Fernandes AY. Periodontal effects of rapid maxillary expansion with tooth-tissue-borne and tooth-borne expanders: a computed tomography evaluation. Am J Orthod Dentofac Orthop. 2006;129(6):749–58.
5. Chamberland S, Proffit WR. Short-term and long-term stability of surgically assisted rapid palatal expansion revisited. Am J Orthod Dentofac Orthop. 2011;139(6):815–e221.
6. Koudstaal MJ, Poort LJ, van der Wal KGH, Wolvius EB, Prahl-Andersen B, Schulten AJM. Surgically assisted rapid maxillary expansion (SARME): a review of the literature. Int J Oral Maxillofac Surg. 2005;34(7):709–14.
7. Suri L, Taneja P. Surgically assisted rapid palatal expansion: a literature review. Am J Orthod Dentofac Orthop. 2008;133(2):290–302.
8. Claeys G, Vinayahalingam S, Kleinheinz J, Bergé S, Xi T. Does expander design influence the risk of asymmetric palatal expansion? A retrospective cohort study. Head Face Med. 2025;21(1):60.

9. Huizinga MP, Meulstee JW, Dijkstra PU, Schepers RH, Jansma J. Bone-borne surgically assisted rapid maxillary expansion: A retrospective three-dimensional evaluation of the asymmetry in expansion. J Cranio-Maxillofacial Surg. 2018;46(8):1329–35.
10. Carvalho PHA, Moura LB, Trento GS, Holzinger D, Gabrielli MAC, Gabrielli MFR, et al. Surgically assisted rapid maxillary expansion: a systematic review of complications. Int J Oral Maxillofac Surg. 2020;49(3):325–32.
11. Alkhayer A, Piffkó J, Lippold C, Segatto E. Accuracy of virtual planning in orthognathic surgery: a systematic review. Head Face Med. 2020;16(1):34.
12. Ho C-T, Lin H-H, Liou EJW, Lo L-J. Three-dimensional surgical simulation improves the planning for correction of facial prognathism and asymmetry: A qualitative and quantitative study. Sci Rep. 2017;7(1):40423.
13. Heufelder M, Wilde F, Pietzka S, Mascha F, Winter K, Schramm A, et al. Clinical accuracy of waferless maxillary positioning using customized surgical guides and patient specific osteosynthesis in bimaxillary orthognathic surgery. J Craniomaxillofac Surg. 2017;45(9):1578–85.
14. Viet H, Marya A, Apuzzo Fd, Nucci L. The clinical applications and outcomes of digital MARPE in orthodontics: A scoping review. Semin Orthod. 2025;31(2):299–309.
15. Jara S, Thuler E, Hutz M, Yu J, Cheong C, Boucher N, et al. Posterior Palatal Expansion via Subnasal Endoscopy (2PENN) for Maxillary Deficiency: A Pilot Study. Laryngoscope. 2023;134:1970–7.
16. World Medical Association Declaration of Helsinki. : ethical principles for medical research involving human subjects. J Am Coll Dent. 2014;81(3):14–8.
17. Vandenbroucke JP, von Elm E, Altman DG, Gotzsche PC, Mulrow CD, Pocock SJ, et al. Strengthening the Reporting of Observational Studies in Epidemiology (STROBE): explanation and elaboration. Int J Surg. 2014;12(12):1500–24.
18. Rana M, Buchbinder D, Aniceto GS, Mast G. Patient-Specific Solutions for Cranial, Midface, and Mandible Reconstruction Following Ablative Surgery: Expert Opinion and a Consensus on the Guidelines and Workflow. Craniomaxillofac Trauma Reconstr. 2025;18(1):15.
19. Gellrich N-C, Rahlf B, Zimmerer R, Pott P-C, Rana M. A new concept for implant-borne dental rehabilitation; how to overcome the biological weak-spot of conventional dental implants? Head Face Med. 2017;13(1):17.
20. Savoldelli C, Vandersteen C, Dassonville O, Santini J. Dental occlusal-surface-supported titanium guide to assist cutting and drilling in mandibular bilateral sagittal split osteotomy. J Stomatology Oral Maxillofacial Surg. 2018;119(1):75–8.
21. Naziri E, Schramm A, Wilde F. Accuracy of computer-assisted implant placement with insertion templates. GMS Interdiscip Plast Reconstr Surg DGPW. 2016;5:Doc15.
22. Scheurer M, Schulze J, Lins T, Daut T, Kasper R, Wilde F, et al. Mandibular positioning using patient-specific guides and osteosynthesis implants in bimaxillary orthognathic surgery with maxilla-first approach. A 3D-analysis. J Craniomaxillofac Surg. 2025;53(11):1935–45.

23. Fedorov A, Beichel R, Kalpathy-Cramer J, Finet J, Fillion-Robin JC, Pujol S, et al. 3D Slicer as an image computing platform for the Quantitative Imaging Network. Magn Reson Imaging. 2012;30(9):1323–41.
24. Probst FA, Cornelius CP, Otto S, Malenova Y, Probst M, Liokatis P, et al. Accuracy of free-hand positioned patient specific implants (PSI) in primary reconstruction after inferior and/or medial orbital wall fractures. Comput Biol Med. 2021;137:104791.
25. Crum WR, Camara O, Hill DL. Generalized overlap measures for evaluation and validation in medical image analysis. IEEE Trans Med Imaging. 2006;25(11):1451–61.
26. Taha AA, Hanbury A. Metrics for evaluating 3D medical image segmentation: analysis, selection, and tool. BMC Med Imaging. 2015;15:29.
27. Badiali G, Bevini M, Ruggiero F, Cercenelli L, Lovero E, De Simone E, et al. Validation of a patient-specific system for mandible-first bimaxillary surgery: ramus and implant positioning precision assessment and guide design comparison. Sci Rep. 2020;10(1):13317.
28. Pietzka S, Fink J, Winter K, Wilde F, Schramm A, Ebeling M et al. Dental Root Injuries Caused by Osteosynthesis Screws in Orthognathic Surgery-Comparison of Conventional Osteosynthesis and Osteosynthesis by CAD/CAM Drill Guides and Patient-Specific Implants. J Pers Med. 2023;13(5).
29. Wilde F, Cornelius CP, Schramm A. Computer-Assisted Mandibular Reconstruction using a Patient-Specific Reconstruction Plate Fabricated with Computer-Aided Design and Manufacturing Techniques. Craniomaxillofac Trauma Reconstr. 2014;7(2):158–66.
30. van Eijnatten M, van Dijk R, Dobbe J, Streekstra G, Koivisto J, Wolff J. CT image segmentation methods for bone used in medical additive manufacturing. Med Eng Phys. 2018;51:6–16.

# Figures

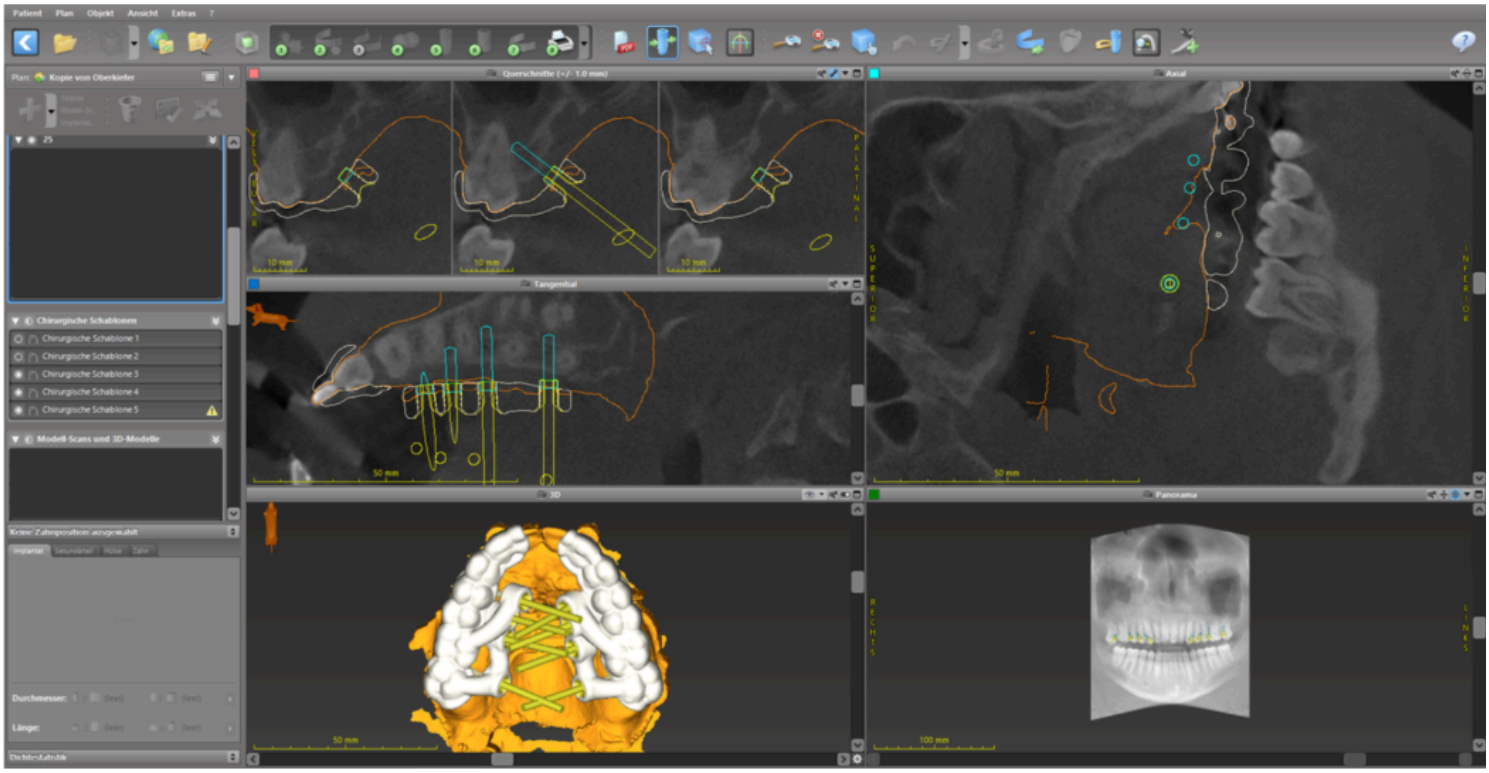


**Figure 1**

VSP of patient-specific SARPE device (PSSD) positioning based on CBCT and intraoral scan data. Multiplanar visualization of a fully digital backward-planning workflow for SARPE. Upper row: Coronal views demonstrating the virtual positioning of titanium drill sleeves (yellow) in relation to adjacent anatomical structures. Planned screw trajectories (light blue) are oriented along available cortical bone while avoiding dental root structures. Middle row: Axial reconstructions enabling detailed assessment of spatial alignment, screw angulation and planned screw length, with verification of safe intraosseous positioning within the maxilla. Lower row: 3D reconstruction of the maxilla with superimposed planned screw trajectories and the patient-specific drilling guide (PSDG), complemented by a panoramic projection illustrating the overall distribution and number of planned screws.

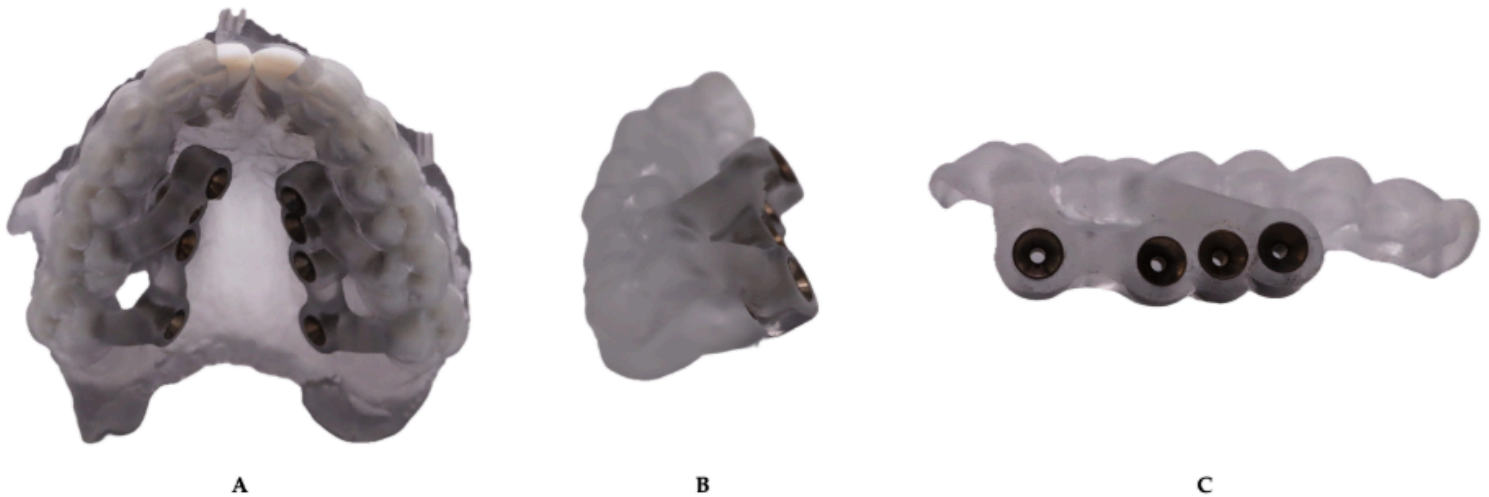


**Figure 2**

PSDG for guided placement of the patient-specific SARPE device. (A) Occlusal view of the dentition-supported, additively manufactured PSDG demonstrating its bilateral design and precise adaptation to the maxillary dental arch. Integrated metallic drill sleeves define the planned screw trajectories for guided transmucosal drilling. (B) Lateral view illustrating the vertical offset and spatial relationship between the guide body and the sleeve-bearing fixation segment, enabling controlled access within the anatomically constrained palatal vault. (C) Side view of the quadrant-specific guide segment showing the sequential arrangement of the drill sleeves corresponding to the virtually planned screw positions. The sleeves provide predefined angulation and depth control for accurate transfer of the virtual surgical plan to the operative field.

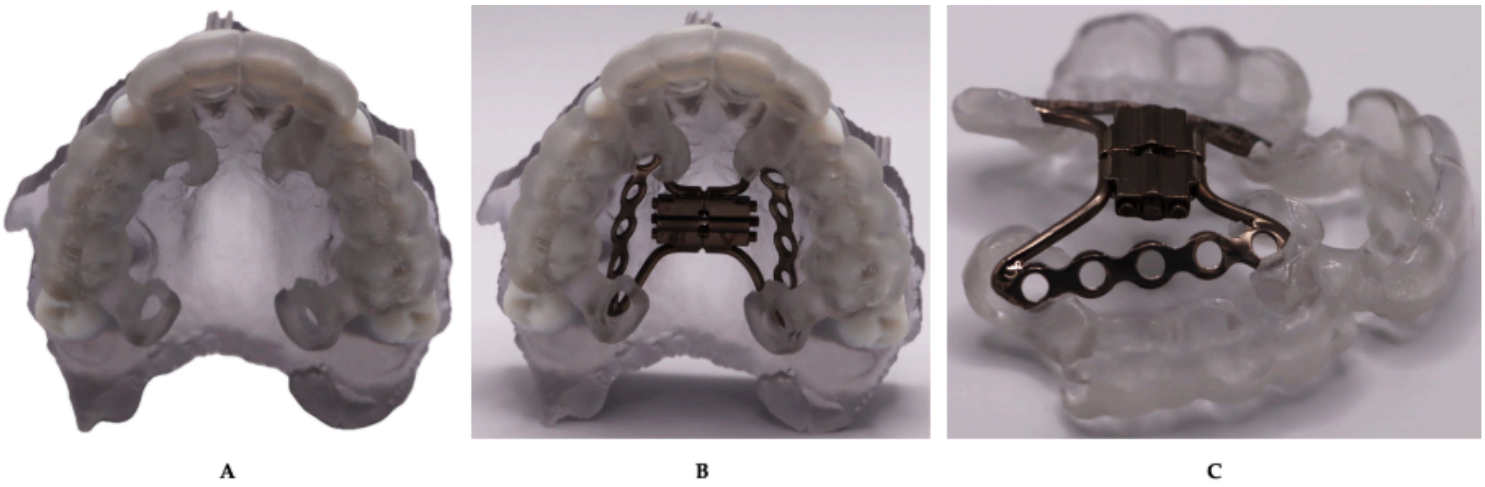



**Figure 3**

PSPG for guided positioning of the PSSD. (A) Occlusal view of the additively manufactured, dentition-supported PSPG demonstrating precise anatomical adaptation to the maxillary dental arch and palatal vault. (B) PSPG with inserted PSSD illustrating the predefined spatial relationship between guide and device. (C) Lateral view highlighting the interface between the PSPG and the PSSD.

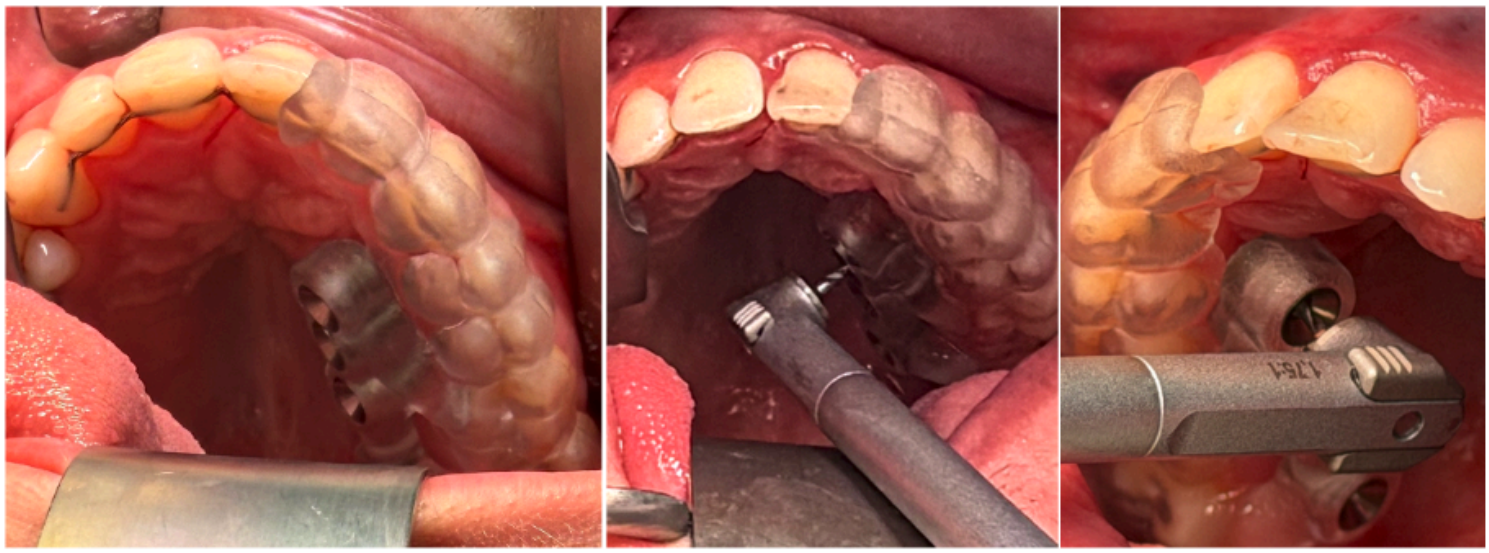



**Figure 4**

Guided osteosynthesis preparation using PSDG. (A) Intraoral view showing quadrant-specific insertion of the dentition-supported PSDG with accurate seating and high positional stability along the maxillary dental arch. (B) Transmucosal template-guided drilling was performed through the integrated titanium drill sleeves. (C) Detailed intraoperative view demonstrating controlled drill angulation and access within the anatomically confined palatal vault, ensuring accurate execution of the VSP.

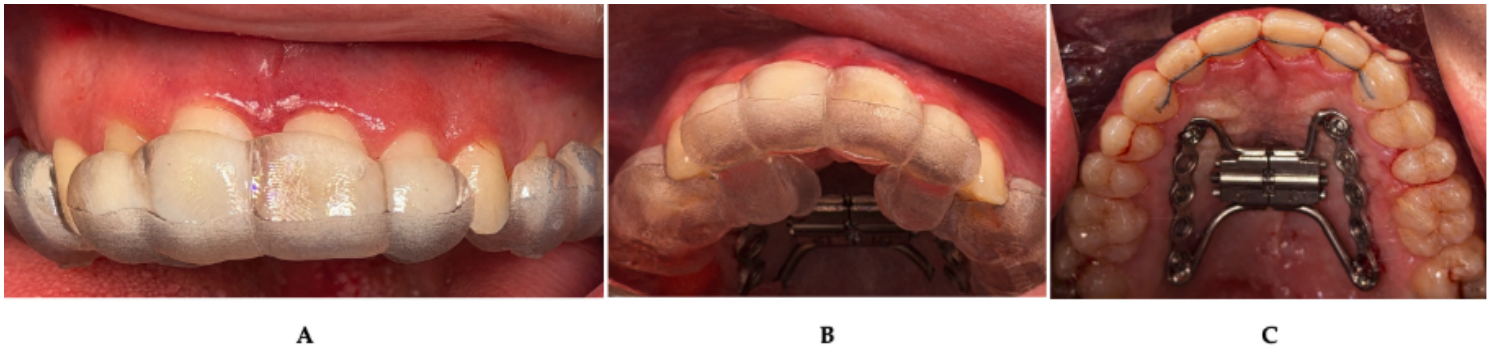



**Figure 5**

Guided insertion of the PSSD using the PSPG. (A) Intraoral frontal view demonstrating dentition-supported seating of the 3D-printed PSPG. (B) Occlusal view illustrating guided insertion of the PSSD through the PSPG, enabling transfer of the VSP to the palatinal vault (C) Intraoperative situation after PSPG removal, showing the correctly positioned PSSD fixed to the palatal vault using locking screws.

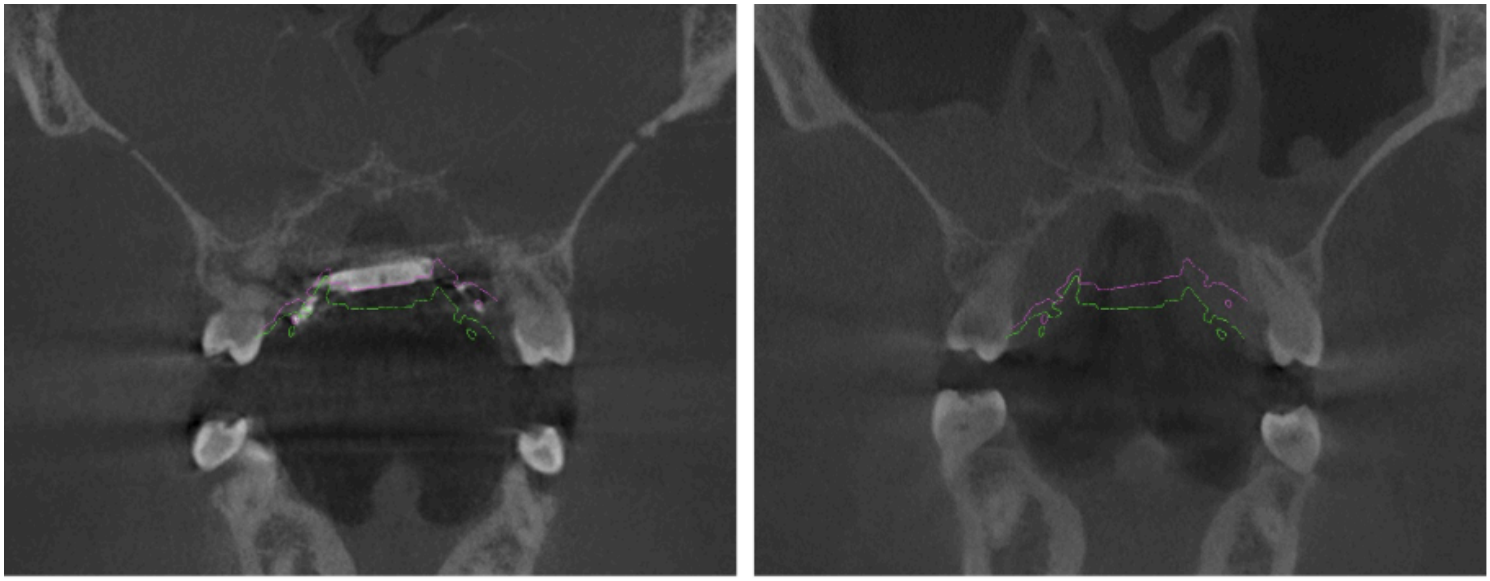



**Figure 6**

CBCT-based evaluation of planned versus postoperative PSSD position. (A) Coronal CBCT slice with superimposed virtually planned PSSD (green) and postoperative achieved position (magenta), demonstrating overall spatial correspondence in the central palatal region, with a progressive cranial deviation observed in the second quadrant. (B) Corresponding coronal CBCT slice illustrating regional deviations between planned and achieved device positioning, with discrepancies primarily located at the lateral fixation arms in the second quadrant. These superimpositions are based on rigid registration of CBCT datasets and were used in combination with intraoral surface registration to assess the spatial relationship between the virtually planned and postoperative PSSD position.

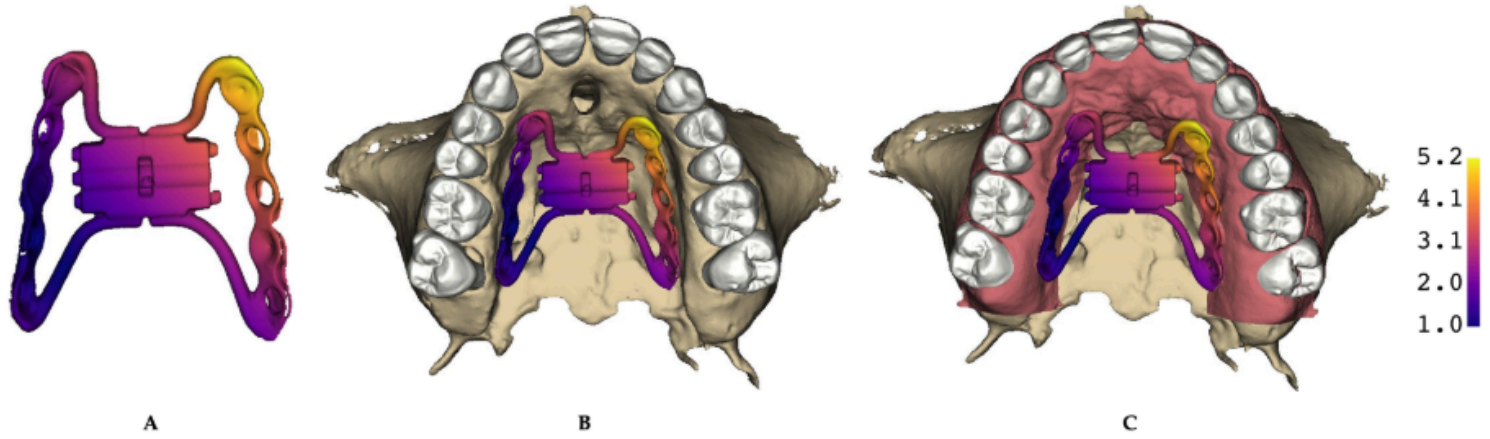



**Figure 7**

3D accuracy analysis of PSSD positioning based on CBCT and intraoral surface registration. (A) Color-coded surface distance map illustrating the geometric deviation between the virtually planned and the postoperative PSSD position. The color scale (right) represents point-to-surface distances (mm), with lower deviations shown in dark blue/purple and higher deviations in yellow. (B) Superimposition of the

planned PSSD onto the postoperative maxillary model, demonstrating overall spatial correspondence, particularly in the central expansion screw region and in the posterior region of the first quadrant. (C) Combined visualization including dentition and soft tissue surface from intraoral scan registration, highlighting the spatial relationship between the PSSD and the maxillary anatomy.